Journal of Materials and Engineering Structures

Research Paper

The Computer Algorithm for Machine Equations of Classical Distribution

Florian Ion T. Petrescu [a],*, Relly Victoria Petrescu [a], MirMilad Mirsayar [b]

[a]*Bucharest Polytechnic University, 060042 Bucharest, (CE) Romania*

[b]*Texas A&M University, College Station, TX (Texas), USA*

A B S T R A C T

This paper presents an algorithm for setting the dynamic parameters of the classical distribution mechanism of the internal combustion engines. One presents the dynamic, original, machine motion equations. The equation of motion of the machine that generates the angular speed of the camshaft (which varies with position and rotation speed) is obtained by conservation kinetic energy of the machine. An additional variation of angular speed is added by multiplying by the coefficient dynamic D (generated by the forces out of mechanism and or by the forces generated by the elasticity of the system). Kinetic energy conservation shows angular speed variation (from the camshaft) with inertial masses, while the dynamic coefficient introduces the variation of w with forces acting in the mechanism. Deriving the first equation of motion of the machine we obtain the second equation of motion dynamic. From the second equation of motion of the machine, we determine the angular acceleration of the camshaft. It shows the distribution of the forces on the camshaft mechanism to the internal combustion heat engines. Dynamic, the velocities can be distributed in the same way as forces. Practically, in the dynamic regimes, the velocities have the same timing as the forces. Calculations should be made for an engine with a single cylinder.

1   Introduction

In conditions which started to magnetic motors, oil fuel is decreasing, energy which was obtained by burning oil is replaced with nuclear energy, hydropower, solar energy, the wind, and other types of unconventional energy, in the conditions in which electric motors have been instead of internal combustion in public transport, but more recently they have entered in the cars world (Honda has produced a vehicle that uses a compact electric motor and electricity consumed by the battery is restored to a system that uses an electric generator with hydrogen combustion in cells, so we have a car that burns hydrogen, but has an electric motor), which is the role and prospects which have internal combustion engines type Otto or Diesel?

---

* Corresponding author. Tel.: +40724040348.
E-mail address: fitpetrescu@gmail.com

Internal combustion engines in four-stroke (Otto, Diesel) are robust, dynamic, compact, powerful, reliable, economic, autonomous, independent and will be increasingly clean [1-15].

Let's look at just remember that any electric motor that destroys ozone in the atmosphere needed our planet by sparks emitted by collecting brushes. The immediate consequence is that if we only use electric motors in all sectors, we'll have problems with higher ozone shield that protects our planet and without which no life could exist on Earth. Magnetic motors (combined with the electromagnetic) are just in the beginning, but they offer us a good perspective, especially in the aeronautics industry. Probably at the beginning, they will not be used to act as a direct transmission but will generate electricity that will fill the battery that will actually feed the engine (probably an electric motor).

The Otto engines or those with internal combustion, in general, will have to adapt to hydrogen fuel. It is composed of the basic (hydrogen) can extract industrially, practically from any item (or combination) through nuclear, chemical, photonic by radiation, by burning, etc... (Most easily hydrogen can be extracted from water by breaking up into constituent elements, hydrogen and oxygen by burning hydrogen one obtains water again that restores a circuit in nature, with no losses and no pollution). Hydrogen must be stored in reservoirs cell (a honeycomb) for there is no danger of explosion the best would be if we could breaking up water directly on the vehicle, in which case the reservoir would feed water (and there were announced some successful).

As a backup, there are trees that can donate a fuel oil, which could be planted in the extended zone, or directly in the consumer court. With many years ago, Professor Melvin Calvin, (Berkeley University), discovered that "Euphora" tree, a rare species, contained in its trunk a liquid that has the same characteristics as raw oil. The same professor discovered on the territory of Brazil, a tree which contains in its trunk a fuel with properties similar to diesel [16-39]. During a journey in Brazil, the natives drove him (Professor Calvin) to a tree called by them "Copa-Iba". At the time of boring the tree trunk, from it to begin flow a gold liquid, which was used as an indigenous raw material base for the preparation of perfumes or, in concentrated form, as a balm. Nobody sees that it is a pure fuel that can be used directly by diesel engines. Calvin said that after he poured the liquid extracted from the tree trunk directly into the tank of his car (equipped with a diesel), engine functioned irreproachably. In Brazil, the tree is fairly widespread. It could be adapted in other areas of the world, planted in the forests, and the courts of people. From a jagged tree is filled about half of the tank one covers the slash and it is not open until after six months it means that having 12 trees in a courtyard, a man can fill monthly a tank with the new natural diesel fuel.

In some countries (USA, Brazil and Germany) producing alcohol or vegetable oils, for their use as fuel. In the future, aircraft will use ion engines, magnetic, laser or various microparticles accelerated. Now, and the life of the jet engine begin to end. Even in these conditions, internal combustion engines will be maintained in land vehicles (at least), for power, reliability and especially their dynamics. Thermal engine efficiency is still low and, about one-third of the engine power is lost just by the distribution mechanism. Mechanical efficiency of cam mechanisms was about 4-8%. In the past 20 years, managed to increase to about 14-18%, and now is the time to pick it up again at up to 60%. This is the main objective of this paper.

2   The state of the art

In 1680, Dutch physicist Christian Huygens designs the first internal combustion engine. In 1807, the Swiss Francois Isaac de Rivaz invented an internal combustion engine that uses a liquid mixture of hydrogen and oxygen as fuel. However, Rivaz's engine for its new engine has been a major failure, so its engine has passed to the deadline, with no immediate application. In 1824, English engineer Samuel Brown adapted a steam engine to make it work with gasoline. In 1858, the Belgian engineer Jean Joseph Etienne Lenoir invented and patented two years later, the first real-life internal combustion engine with spark-ignition, liquid gas (extracted from coal), a two-stroke engine. In 1863, all Belgian Lenoir is adapting a carburettor to his engine by making it work with oil (or gasoline). In 1862, the French engineer Alphonse Beau de Rochas first patented the four-stroke internal combustion engine (but without building it).

It is the merit of the German engineers Eugen Langen and Nikolaus August Otto to build (physically, practically the theoretical model of the French Rochas), the first four-stroke internal combustion engine in 1866, with electric ignition, charging and distribution in a form Advanced. Ten years later (in 1876), Nikolaus August Otto patented his engine. In the same year (1876), Sir Dougald Clerk, the two-time engine of the Belgian Lenoir, (bringing it to the shape known today). In

1885, Gottlieb Daimler arranges a four-stroke internal combustion engine with a single vertical cylinder and an improved carburetor.

A year later, his compatriot Karl Benz brings some improvements to the four-stroke gasoline engine. Both Daimler and Benz were working new engines for their new cars (so famous). In 1889, Daimler improves the four-stroke internal combustion engine, building a "two cylinder in V", and bringing the distribution to today's classic form, "with mushroom-shaped valves". In 1890, Wilhelm Maybach, builds the first four-cylinder four-stroke internal combustion. In 1892, German engineer Rudolf Christian Karl Diesel invented the compression-ignition engine, in short the diesel engine.

The first valve mechanisms appeared in 1844, being used in steam locomotives they were designed and built by the Belgian mechanical engineer Egide Walschaerts. The first cam mechanisms are used in England and the Netherlands in the wars. In 1719, in England, some John Kay opens in a five-story building a filth. With a staff of over 300 women and children, this would be the world's first factory. He also becomes famous by inventing the flying sail, which makes the tissue much faster. But the machines were still manually operated. It was not until 1750 that the textile industry was to be revolutionized by the widespread application of this invention. Initially the weavers opposed it, destroying flying sails and banishing the inventor. By 1760, the wars and the first factories appeared in the modern sense of the word. It took the first engines. For over a century, Italian Giovanni Branca had proposed the use of steam to drive turbines. Subsequent experiments were not satisfying. In France and England, brand inventors, like Denis Papin or the Worcester Marquis, came up with new ideas. At the end of the seventeenth century, Thomas Savery had already built the "friend of the miner", a steam engine that put into operation a pump to remove water from the galleries. Thomas Newcomen has made the commercial version of the steam pump, and engineer James Watt develops and adapts a speed regulator that improves the engine's net. Together with the manufacturer Mathiew Boulton builds the first steam-powered engines and in less than half a century, the wind that had fueled more than 3,000 years ago, the propulsion power at sea now only inflates the pleasure craft. In 1785 came into operation the first steam driven steamer followed quickly by a few dozen.

The first distribution mechanisms occur with four-stroke engines for cars. Over the past 25 years, a number of variants have been used to increase the number of valves on a cylinder from 2 valves per cylinder to just 12 valves / cylinder but returned to the simpler versions with 2, 3, 4, or 5 valves / cylinder. A larger inlet or outlet area can also be provided with a single valve, but when there is more, a variable spread over a larger speed swim can be achieved.

A distribution mechanism balanced presented by Scania, next-generation, four valves per cylinder, two intake and two exhaust (it returned to the classical mechanism rod pushers and rocker, as the dynamics of this model mechanism is much better than to the non-cobbled model). The Swedish builder even considered that the dynamics of the classic mechanism used by replacing the classic stick with the sole by roller can be improved. The modular combustion chamber has a unique construction of the valve actuator. The valve springs exert great forces to ensure their rapid closure. The forces for their opening are provided by camshaft driven camshafts. Pulleys and cams are large, ensuring smooth and precise action on the valves. This is reflected in the low fuel consumption. The accuracy of the distribution mechanism is a vital factor in engine efficiency and clean combustion. An important benefit brought by the size of the tachets is the low rate of wear. This reduces the need for adjustments. The operation of the valves remains constant for a long period of time. If adjustments are required, they can be made quickly and easily.

The Peugeot Citroën Group in 2006 built a 4-valve hybrid engine with 4 cylinders the first cam opens the normal valve and the second with the phase shift. Almost all current models have stabilized at four valves per cylinder to achieve a variable distribution. In 1971, K. Hain proposes a method of optimizing the cam mechanism to obtain an optimal (maximum) transmission angle and a minimum acceleration [40] at the output. In 1979, F. Giordano investigates the influence of measurement errors in the kinematic analysis of the camel [41].

In 1985, P. Antonescu presented an analytical method for the synthesis of the cam mechanism and the flat barbed wire [42], and the rocker mechanism [43]. In 1988, J. Angeles and C. Lopez-Cajun presented the optimal synthesis of the cam mechanism and oscillating plate stick [44]. In 2001 Dinu Taraza analyzes the influence of the cam profile, the variation of the angular speed of the distribution shaft and the power, load, consumption and emission parameters of the internal combustion engine [45]. In 2005, Petrescu and Petrescu, R., present a method of synthesis of the rotating camshaft profile with rotary or rotatable tappet, flat or roller, in order to obtain high yields at the exit [33-34].

In the paper [46], there is presented a basic, single-degree, dual-spring model with double internal damping for simulating the motion of the cam and punch mechanism. In the paper [47] is presented the basic dynamic model of a cam

mechanism, stick and valve, with two degrees of freedom, without internal damping. A dynamic model with both damping in the system, external (valve spring) and internal one is the one presented in the paper [48]. A dynamic model with a degree of freedom, generalized, is presented in the paper [49], in which there is also a two-degree model with double damping. In the paper [50] is proposed a dynamic model with 4 degrees of freedom, obtained as follows: the model has two moving masses these by vertical vibration each impose a degree of freedom one mass is thought to vibrate and transverse, generating yet another degree of freedom and the last degree of freedom is generated by torsional torsion of the camshaft. Also in the paper [50] is presented a simplified dynamic model, amortized amortization. Also in [50] there is also a dynamic model, which also takes into account the torsional vibrations of the camshaft. A dynamic model with four degrees of freedom is presented in the paper [51], with a single moving oscillating mass, representing one of the four degrees of freedom. The other three freedoms result from a torsional deformation of the camshaft, a vertical bending (z), camshaft and a bending strain of the same shaft, horizontally (y), all three deformations, in a plane perpendicular to the axis of rotation. In the papers [2] and [52] there are presented two dynamic models with internal damping of the system, c, variable. Determining the internal damping of the system, c, is based on the comparison between the dynamic equation coefficients, written in two different ways, Newtonian and Lagrangian.

3 Determining the first equation of machine

One presents the dynamic, original, machine motion equations. The equation of motion of the machine that generates the angular speed of the shaft (which varies with position and rotation speed) is obtained by conservation kinetic energy of the machine. An additional variation of angular speed is added by multiplying by the coefficient dynamic (generated by the forces out of mechanism).

Kinetic energy conservation shows angular speed variation (from the main shaft) with inertial masses, while the dynamic coefficient introduces the variation of w with forces acting in the mechanism [16-39].

In system (1) one determines the variable rotation velocity of the (cam) shaft, in function of the position φ of the shaft, and of rotation nominal speed ω_m. One starts from the equation of kinetics energy (that is conserved).

$$
\begin{cases}
\dfrac{1}{2} \cdot J_m^* \cdot \omega_m^2 = \dfrac{1}{2} \cdot J_{max}^* \cdot \omega_{min}^2 = \\[2mm]
= \dfrac{1}{2} \cdot J_{min}^* \cdot \omega_{max}^2 = \dfrac{1}{2} \cdot J^* \cdot \omega^2 \Rightarrow \\[2mm]
\Rightarrow J_m^* \cdot \omega_m^2 = J_{max}^* \cdot \omega_{min}^2 = J_{min}^* \cdot \omega_{max}^2 = J^* \cdot \omega^2 \\[2mm]
\Rightarrow J_m^* \cdot \omega_m^2 = J^* \cdot \omega^2 \\[2mm]
\omega^2 = \dfrac{J_m^*}{J^*} \cdot \omega_m^2; \quad \omega = \sqrt{\dfrac{J_m^*}{J^*}} \cdot \omega_m \\[4mm]
J_m^* = \dfrac{J_{max}^* + J_{min}^*}{2} \\[3mm]
\omega_m \equiv \omega_{med} \equiv \omega_n = 2 \cdot \pi \cdot \nu = 2\pi \cdot \dfrac{n}{60} = \dfrac{\pi}{30} \cdot n \\[3mm]
\omega^2 = \dfrac{J_m^*}{J^*} \cdot \omega_m^2 \\[3mm]
\omega = \sqrt{\dfrac{J_m^*}{J^*}} \cdot \omega_m
\end{cases}
\tag{1}
$$

The first movement equation of the machine takes the initial forms (2):

$$
\begin{cases}
\omega^2 = \dfrac{J_m^*}{J^*} \cdot \omega_m^2 \\[3mm]
\omega = \sqrt{\dfrac{J_m^*}{J^*}} \cdot \omega_m
\end{cases}
\tag{2}
$$

Since J* is a function of the angle φ and ω_n is a function of n, it follows that ω is a function of angle φ and angular rotation speed n=> $\omega = \omega(\varphi, n)$.

An additional variation of angular speed is added by multiplying by the coefficient dynamic (generated by the forces from mechanism and out of mechanism). The final forms of the first movement equation of the machine can be seen in the system (3).

$$\begin{cases} \omega^2 = \dfrac{J_m^*}{J^*} \cdot \omega_m^2 \cdot D^2 \\[3mm] \omega = \sqrt{\dfrac{J_m^*}{J^*}} \cdot \omega_m \cdot D \end{cases} \tag{3}$$

Generally the coefficient D has two components, the first one (Dc) generated by the forces from couples, and the second one generated by the elasticity forces of the system (De).

Dc was already presented in more published articles, but its influence on dynamics of classical distribution is insignificant. For this reason in this paper we'll present only the new coefficient, De, which introducing the elasticity effect of the system. In all older articles this important effect was treated separately by integrating the equations of motion Lagrange or Newton. Dynamic equation obtained for the system elasticity effect was complicated. But the main reason for introducing this coefficient is that the authors want all the dynamic influences of system can be introduced as a dynamic factor. Even the effect of inertial forces (the masses system) appears as a dynamic factor (see the system 4). In this way all the dynamic influences appear as a change produced to the input angular velocity [36].

$$\begin{cases} D_I = \sqrt{\dfrac{J_m^*}{J^*}}; \quad D_c = 1; \quad D_e \\[3mm] D = D_I \cdot D_c \cdot D_e; \quad D^2 = D_I^2 \cdot D_c^2 \cdot D_e^2 \\[3mm] \omega^2 = \omega_m^2 \cdot D^2; \quad \omega = \omega_m \cdot D \end{cases} \tag{4}$$

4   Determining the second equation of machine

The second machine equation is determined by the derivation of the first machine equation in function of the time (see the system 5).

$$\begin{cases} D = D_I \cdot D_c \cdot D_e; \quad D^2 = D_I^2 \cdot D_c^2 \cdot D_e^2 \\[2mm] D' = D_I^l \cdot D_c \cdot D_e + D_I \cdot D_c^l \cdot D_e + D_I \cdot D_c \cdot D_e^l \\[3mm] \omega^2 = D^2 \cdot \omega_m^2; \omega = D \cdot \omega_m; \varepsilon = D' \cdot \omega \cdot \omega_m = D' \cdot D \cdot \omega_m^2 \\[3mm] \begin{cases} \varepsilon = D_I \cdot D_I^l \cdot D_c^2 \cdot D_e^2 \cdot \omega_m^2 + D_I^2 \cdot D_c \cdot D_c^l \cdot D_e^2 \cdot \omega_m^2 + \\ +D_I^2 \cdot D_c^2 \cdot D_e \cdot D_e^l \cdot \omega_m^2 \end{cases} \\[5mm] D_I = \sqrt{\dfrac{J_m^*}{J^*}}; \quad D_I^2 = \dfrac{J_m^*}{J^*}; \quad D_I \cdot D_I^l = -\dfrac{J_m^* \cdot J^{*l}}{2 \cdot J^{*2}} \\[5mm] \begin{cases} \varepsilon \cdot J^* + \dfrac{1}{2}\omega^2 \cdot J^{*l} = M_m^* - M_r^* \\ M_m^* - M_r^* = J_m^* \cdot \omega_m^2 \cdot (D_c \cdot D_c^l \cdot D_e^2 + D_c^2 \cdot D_e \cdot D_e^l) \end{cases} \end{cases} \tag{5}$$

5 Application to the Otto engine classical distribution

One determines now the dynamics of the classical distribution at an Otto engine (Fig. 1) by an original method [37-38].
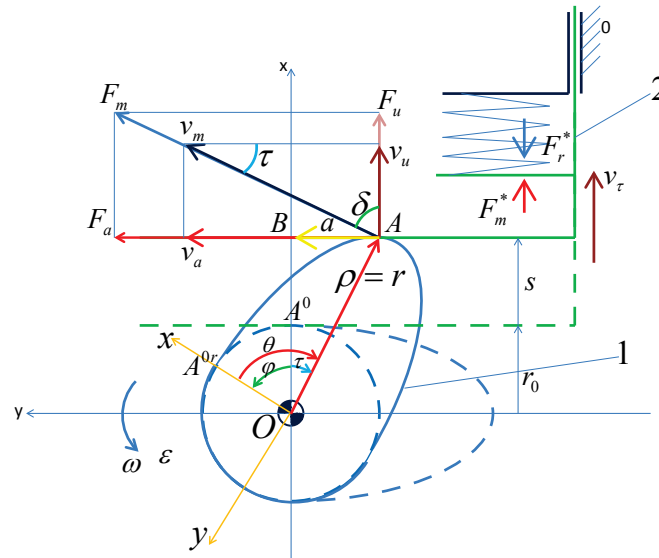

Fig. 1. Classical distribution

First of all one determines the motor and resistant forces (system 6) reduced at the axis of the follower.

$$
\begin{cases}
F_m^* = K \cdot (y - x) = K \cdot (s - x) \Rightarrow M_m = K \cdot (s - x) \cdot s' \\
F_r^* = k \cdot (x_0 + x) \Rightarrow M_r = k \cdot (x_0 + x) \cdot x' \\
\text{assuming static: } F_m = F_r \Rightarrow \\
\Rightarrow \begin{cases}
x = \dfrac{K}{K+k} \cdot s - \dfrac{k}{K+k} \cdot x_0; \quad x' = \dfrac{K}{K+k} \cdot s' \\
s = \dfrac{K+k}{K} \cdot x + \dfrac{k}{K} \cdot x_0; \quad s' = \dfrac{K+k}{K} \cdot x'
\end{cases} \\
\begin{cases}
M_m^* = K \cdot s \cdot s' - (K+k) \cdot x \cdot x' \\
M_r^* = k \cdot x_0 \cdot x' + k \cdot x \cdot x'
\end{cases} \Rightarrow \\
M^* = M_m - M_r = K \cdot s \cdot s' - (K + 2k) \cdot x \cdot x' - k \cdot x_0 \cdot x'
\end{cases}
\tag{6}
$$

Now identify the reduced moment of systems 5 and 6 and we obtain the relations of the system 7 (with $D_c = 1$ and $D_c' = 0$).

$$
\begin{cases}
J_m^* \cdot \omega_m^2 \cdot D_e \cdot D_e^l = K \cdot s \cdot s' - (K + 2k) \cdot x \cdot x' - k \cdot x_0 \cdot x \\
D_e \cdot D_e^l = \dfrac{K}{J_m^* \cdot \omega_m^2} \cdot s \cdot s' - \dfrac{K + 2k}{J_m^* \cdot \omega_m^2} \cdot x \cdot x' - \dfrac{k \cdot x_0}{J_m^* \cdot \omega_m^2} \cdot x' \\
D_e^2 = \dfrac{K}{J_m^* \cdot \omega_m^2} \cdot s^2 - \dfrac{K + 2k}{J_m^* \cdot \omega_m^2} \cdot x^2 - \dfrac{2k \cdot x_0}{J_m^* \cdot \omega_m^2} \cdot x \\
D_e = \sqrt{\dfrac{K}{J_m^* \cdot \omega_m^2} \cdot s^2 - \dfrac{K + 2k}{J_m^* \cdot \omega_m^2} \cdot x^2 - \dfrac{2k \cdot x_0}{J_m^* \cdot \omega_m^2} \cdot x} \\
D_e^l = \dfrac{\dfrac{K}{J_m^* \cdot \omega_m^2} \cdot s \cdot s' - \dfrac{K + 2k}{J_m^* \cdot \omega_m^2} \cdot x \cdot x' - \dfrac{k \cdot x_0}{J_m^* \cdot \omega_m^2} \cdot x}{\sqrt{\dfrac{K}{J_m^* \cdot \omega_m^2} \cdot s^2 - \dfrac{K + 2k}{J_m^* \cdot \omega_m^2} \cdot x^2 - \dfrac{2k \cdot x_0}{J_m^* \cdot \omega_m^2} \cdot x}}
\end{cases}
\tag{7}
$$

For the classical distribution we still use simplified dynamic relations (system 8).

$$\begin{cases} \omega^2 = \dfrac{J_m^*}{J^*} \cdot \omega_m^2 \cdot D_e^2 \\[2mm] \omega = \sqrt{\dfrac{J_m^*}{J^*}} \cdot \omega_m \cdot D_e \\[2mm] \varepsilon = -\dfrac{1}{2} \dfrac{J^{*l}}{J^*} \cdot \omega^2 + \dfrac{J_m^* \cdot \omega_m^2}{J^*} \cdot D_e \cdot D_e^l \end{cases} \tag{8}$$

It also uses and relationships already known (system 9).

$$\begin{cases} \dot{s} = s' \cdot \omega \\ \ddot{s} = s'' \cdot \omega^2 + s' \cdot \varepsilon \\ \dot{x} = x' \cdot \omega \\ \ddot{x} = x'' \cdot \omega^2 + x' \cdot \varepsilon \\ \begin{cases} x = \rho \cos\theta = \rho \cos(\phi+\tau) = (r_0+s)\cos\phi - s'\sin\phi \\ y = \rho \sin\theta = \rho \sin(\phi+\tau) = (r_0+s)\sin\phi + s'\cos\phi \end{cases} \\ \eta_i = \dfrac{P_u}{P_m} = \dfrac{F_u \cdot v_u}{F_m \cdot v_m} = \dfrac{F_m \cdot \sin\tau \cdot v_m \cdot \sin\tau}{F_m \cdot v_m} = \sin^2\tau \end{cases} \tag{9}$$

For dynamic calculations must be determined: $J^*, J^{*\prime}, J_{Max}^*, J_{min}^*, J_m^*$ (relations system 10).

$$\begin{cases} J^* = J_c + m_T \cdot s'^2 = \dfrac{1}{2} m_c \cdot \rho^2 + m_T \cdot s'^2 = \dfrac{1}{2} m_c \cdot \left[(r_0+s)^2 + s'^2\right] + m_T \cdot s'^2 = \dfrac{1}{2} m_c \cdot (r_0+s)^2 + \left(\dfrac{m_c}{2} + m_T\right) \cdot s'^2 \\ J^{*\prime} = m_c \cdot (r_0+s) \cdot s' + (m_c + 2m_T) \cdot s' \cdot s'' \\ J_{Max}^* = \dfrac{1}{2} m_c \cdot (r_0+h)^2 \\ J_{min}^* = \dfrac{1}{2} m_c \cdot r_0^2 \\ J_m^* \equiv J_{med}^* = \dfrac{1}{2}\left(J_{Max}^* + J_{min}^*\right) = \dfrac{1}{2} m_c \cdot r_0^2 + \dfrac{1}{2} m_c \cdot r_0 \cdot h + \dfrac{1}{4} m_c \cdot h^2 = \dfrac{m_c}{2} \cdot \left(r_0^2 + r_0 \cdot h + \dfrac{h^2}{2}\right) \end{cases} \tag{10}$$

The normal angular velocity of the cam (camshaft) ω_m may be determined with the relation (11).

$$\omega_m = 2 \cdot \pi \cdot v_c = 2\pi \cdot \dfrac{n_c}{60} = \dfrac{\pi \cdot n_c}{30} = \dfrac{\pi \cdot n_m}{60} \tag{11}$$

The dynamic acceleration of the follower can be seen in the figure 2 (h=0.006 [m] r_0=0.013 [m] φ_0=π/2 [rad] m_c=0.2 [kg] m_T=0.1 [kg] n=n_m=5000 [rpm] η=0.305 k=150000 [N/m] x_0=0.03 [m] a=4s). It utilizes cosine law of motion. The cam profile may be seen in the fig. 3.
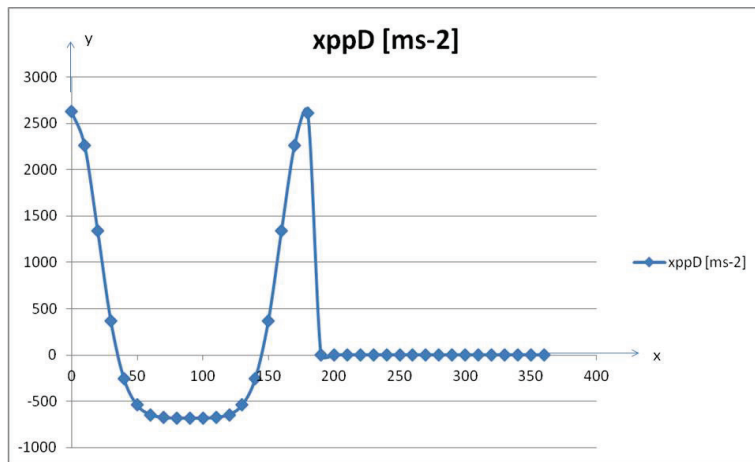
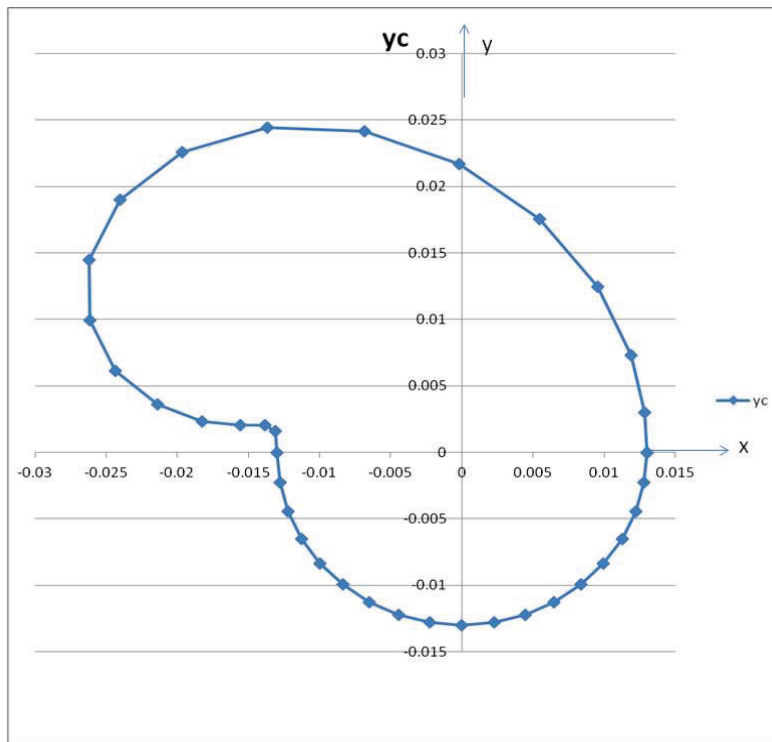*Fig. 2. Classical distribution tappet dynamic acceleration a=4s.*

Fig. 3. Classical distribution cam profile for a=4s η=30%.

-The secret to obtain a high yield consists in summary the AB segment cam with a variable a=4s.

-A more accurate determination of the dynamic acceleration of plunger involves using an old dynamic model that takes into account the elasticity system (relation 12-15).

$$x = s - \frac{(K+k) \cdot m_T \cdot \omega^2 \cdot s'^2 + (k^2 + 2k \cdot K) \cdot s^2 + 2k \cdot x_0 \cdot (K+k) \cdot s}{2 \cdot (K+k)^2 \cdot \left(s + \dfrac{k \cdot x_0}{K+k}\right)} \tag{12}$$

Where x is the dynamic movement of the pusher, while s is its normal, kinematics movement. K is the spring constant of the system, and k is the spring constant of the tappet spring. It note, with x_0 the tappet spring preload, with m_T the mass of the tappet, with ω the angular rotation speed of the cam (or camshaft), where s' is the first derivative in function of φ of the tappet movement, s.
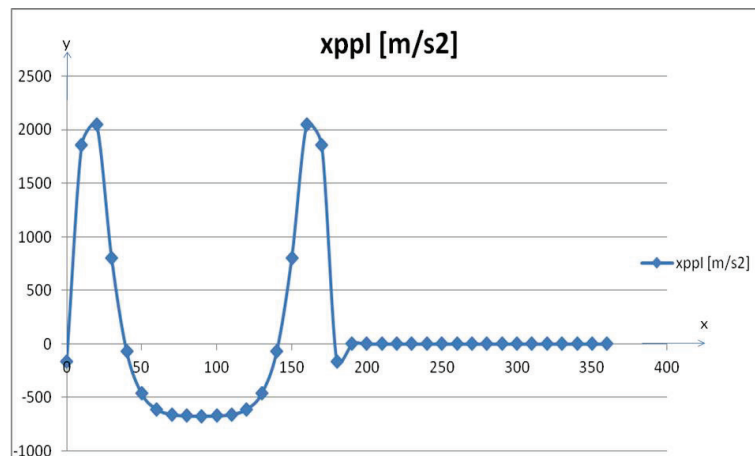
$$\begin{cases} N = (K+k)\cdot m_T \cdot \omega^2 \cdot s'^2 + \\ + (k^2 + 2k\cdot K)\cdot s^2 + 2k\cdot x_0 \cdot (K+k)\cdot s \\ M = \left[(K+k)m_T\omega^2\cdot 2s's'' + \left(k^2 + 2kK\right)\cdot 2ss' + \right. \\ \left. + 2kx_0\left(K+k\right)\cdot s'\right]\cdot\left(s + \dfrac{kx_0}{K+k}\right) - N\cdot s' \\ \\ x' = s' - \dfrac{M}{2\cdot\left(K+k\right)^2\cdot\left(s + \dfrac{kx_0}{K+k}\right)^2} \end{cases} \tag{13}$$

$$\begin{cases} N = (K+k)\cdot m_T \cdot \omega^2 \cdot s'^2 + (k^2 + 2k\cdot K)\cdot s^2 + 2k\cdot x_0 \cdot (K+k)\cdot s \\ M = \left[(K+k)m_T\omega^2\cdot 2s's'' + \left(k^2 + 2kK\right)\cdot 2ss' + 2kx_0\left(K+k\right)\cdot s'\right]\cdot\left(s + \dfrac{kx_0}{K+k}\right) - N\cdot s' \\ \\ O = (K+k)\cdot m_T\cdot\omega^2\cdot 2\cdot\left(s''^2 + s'\cdot s'''\right) + \left(k^2 + 2\cdot k\cdot K\right)\cdot 2\cdot\left(s'^2 + s\cdot s''\right) + 2\cdot k\cdot x_0\cdot(K+k)\cdot s'' \\ \\ x'' = s'' - \dfrac{\left[O\cdot\left(s+\dfrac{kx_0}{K+k}\right) - N\cdot s''\right]\cdot\left(s+\dfrac{kx_0}{K+k}\right) - M\cdot 2\cdot s'}{2\cdot\left(K+k\right)^2\cdot\left(s+\dfrac{kx_0}{K+k}\right)^3} \end{cases} \tag{14}$$

Further the acceleration of the tappet can be determined directly real (dynamic) using the relation (15) (Fig. 4).

$$\ddot{x} = x''\cdot\omega^2 + x'\cdot\varepsilon \tag{15}$$

Fig. 4. Classical distribution tappet real dynamic acceleration obtained with the old dynamic systems: h=0.006 [m] r₀=0.013 [m] φ₀=π/2 [rad] m_c=0.2 [kg] m_T=0.1[kg] n=n_m=5000 [rpm] η=0.305 k=150000 [N/m] x₀=0.03[m].

6   Discussion

The differences between the two systems are small, which certifies the validity of the new dynamic system proposed in the present paper.

The advantages of the new system are obvious: Dynamic equations used are much simpler. The whole dynamic is made based on dynamic coefficients. The dynamic adjustments (made by the new method) seem to be more consistent. They indicate more precisely the required values for x_0 and k. The old system indicates the need for simultaneous growth of these two values to compensate for raising the engine speed. The new one allow only the increase of one parameter or a

limited increase of both, otherwise there is danger of worsening system dynamics. The appearance of the real acceleration can be controlled from the push rod settings (k and x_0).

To obtain an efficiency of 60% at the classical distribution we need to increase the variable length AB (a) from 4s to 12s (see the dynamics in the fig. 5 and the profile on the fig. 6). In this case, I had to double and the spring constant (k=300000 [N/m]).
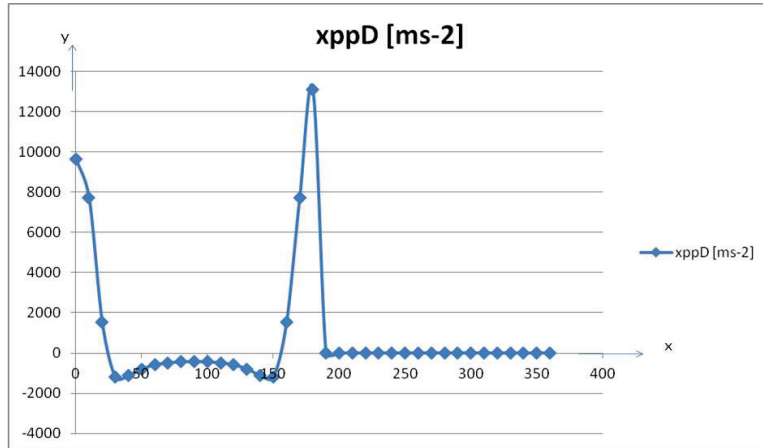

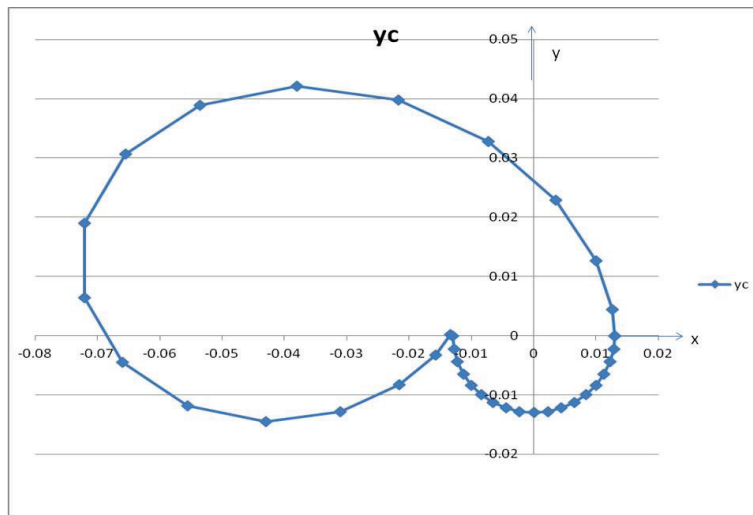**Fig. 5. Classical distribution tappet dynamic acceleration a=12s.**

Fig. 6. Classical distribution cam profile for a=12s η=60%.

7   Presentation of the calculation algorithm of the dynamic synthesis

A rotating cam is basically composed of two concentric circles (a base inner circle, and a top outer circle), connected to each other by two circular arcs as shown in the figure below. There are four main sectors. The ascending (from the base circle to the top circle), the upper station (on the top circle, the RM radius), the descending (return from the peak circle to the base circle), and the last stationary Lower (on the base circle, radius R0). Each sector corresponds to an angle φ, rotating the cam. There are four angles: $\varphi_u, \varphi_{ss}, \varphi_c, \varphi_{si}$. Obviously the sum of the four angles is always 2π [rad], or 360 [deg].

The following values are required: $\varphi_u=\pi/2$ [rad]=90 [deg] $\varphi_{ss}=0$ [rad or deg] $\varphi_c=\pi/2$ [rad]=90 [deg] $\varphi_{si}=\pi$ [rad]=180 [deg] the law of motion cosine both on the climb and on the descent.

The angles $\varphi_u, \varphi_{ss}, \varphi_c, \varphi_{si}$, and the co-axial motion laws for the lifting and descending profile (relations (16) are imposed To the left we have the laws for climb, and to the right for the descent laws].

$$\begin{cases} s = \dfrac{h}{2} - \dfrac{h}{2} \cdot cos\left(\pi \cdot \dfrac{\alpha_u}{\phi_u} \right) & s_c = \dfrac{h}{2} + \dfrac{h}{2} \cdot cos\left(\pi \cdot \dfrac{\alpha_c}{\phi_c} \right) \\[2mm] s' \equiv v_r = \dfrac{\pi \cdot h}{2 \cdot \phi_u} \cdot sin\left(\pi \cdot \dfrac{\alpha_u}{\phi_u} \right) & s_c' = -\dfrac{\pi \cdot h}{2 \cdot \phi_c} \cdot sin\left(\pi \cdot \dfrac{\alpha_c}{\phi_c} \right) \\[2mm] s'' \equiv a_r = \dfrac{\pi^2 \cdot h}{2 \cdot \phi_u^2} \cdot cos\left(\pi \cdot \dfrac{\alpha_u}{\phi_u} \right) & s_c'' = -\dfrac{\pi^2 \cdot h}{2 \cdot \phi_c^2} \cdot cos\left(\pi \cdot \dfrac{\alpha_c}{\phi_c} \right) \\[2mm] s''' \equiv \alpha_r = -\dfrac{\pi^3 \cdot h}{2 \cdot \phi_u^3} \cdot sin\left(\pi \cdot \dfrac{\alpha_u}{\phi_u} \right) & s_c''' = \dfrac{\pi^3 \cdot h}{2 \cdot \phi_c^3} \cdot sin\left(\pi \cdot \dfrac{\alpha_c}{\phi_c} \right) \end{cases} \tag{16}$$

It is required to determine the values of the motion laws of the follower and to plot the motion laws of the follower for a complete rotation of the cam. Here are the diagrams s=s(φ) s'=s'(φ) s''=s''(φ), similar to the model in Figure 7.
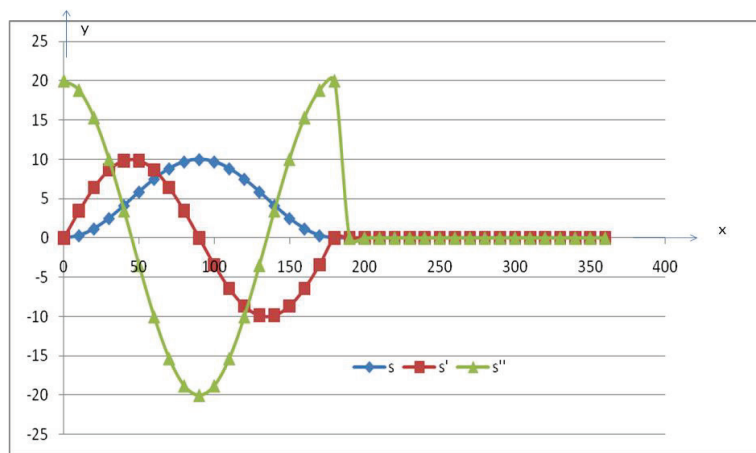

Fig. 7. the diagrams s=s(φ) s'=s'(φ) s''=s''(φ)

Drawing the cam profile is done in Cartesian coordinates, xOy, they are determined for a whole kinematic cycle (360 deg). The relationships (17) are used.

$$\begin{cases} x_C = -s' \cdot cos\,\phi - (r_0 + s) \cdot sin\,\phi \\ y_C = (r_0 + s) \cdot cos\,\phi - s' \cdot sin\,\phi \end{cases} \tag{17}$$

Dynamic synthesis of the rotating camshaft with translatable follower (cosine-cosine law)

Way of working. It determines the laws of motion with relationships (16). One determines A, B and ω² with the relations of the system (18) and ε with expression (19) din (20-23) one determines x, x', x'' şi $\ddot{x}$ [37-38].

$$\begin{cases} \omega^2 = \omega_m^2 \cdot \dfrac{A}{B} \\[2mm] A = M_c \cdot R_0^2 + M_c \cdot \dfrac{h^2}{8} + \dfrac{1}{2} \cdot M_c \cdot R_0 \cdot h + \\[2mm] + \dfrac{1}{8} \cdot M_c \cdot \dfrac{\pi^2 \cdot h^2}{\phi_0^2} + \dfrac{1}{4} \cdot m_T \cdot \dfrac{\pi^2 \cdot h^2}{\phi_0^2} \\[2mm] B = M_c \cdot R_0^2 + M_c \cdot s^2 + 2 \cdot M_c \cdot R_0 \cdot s + M_c \cdot s'^2 + 2 \cdot m_T \cdot s'^2 \\[2mm] \omega_m = 2 \cdot \pi \cdot v_c = 2 \cdot \pi \cdot \dfrac{n_c}{60} = \dfrac{2 \cdot \pi}{60} \cdot \dfrac{n_{motor}}{2} = \dfrac{\pi \cdot n}{60} \end{cases} \tag{18}$$

$$\varepsilon = -\omega^2 \cdot \dfrac{(M_c \cdot s + M_c \cdot R_0 + M_c \cdot s'' + 2 \cdot m_T \cdot s'') \cdot s'}{B} \tag{19}$$

$$x = s - \frac{(K+k) \cdot m_T \cdot \omega^2 \cdot s'^2 + (k^2 + 2k \cdot K) \cdot s^2 + 2k \cdot x_0 \cdot (K+k) \cdot s}{2 \cdot (K+k)^2 \cdot \left(s + \frac{k \cdot x_0}{K+k}\right)} \tag{20}$$

$$\begin{cases} N = (K+k) \cdot m_T \cdot \omega^2 \cdot s'^2 + (k^2 + 2k \cdot K) \cdot s^2 + 2k \cdot x_0 \cdot (K+k) \cdot s \\ M = \left[(K+k)m_T\omega^2 \cdot 2s's'' + (k^2 + 2kK) \cdot 2ss' + 2kx_0(K+k) \cdot s'\right] \cdot \left(s + \frac{kx_0}{K+k}\right) - N \cdot s' \\ x' = s' - \dfrac{M}{2 \cdot (K+k)^2 \cdot \left(s + \frac{kx_0}{K+k}\right)^2} \end{cases} \tag{21}$$

$$\begin{cases} N = (K+k) \cdot m_T \cdot \omega^2 \cdot s'^2 + (k^2 + 2k \cdot K) \cdot s^2 + 2k \cdot x_0 \cdot (K+k) \cdot s \\ M = \left[(K+k)m_T\omega^2 \cdot 2s's'' + (k^2 + 2kK) \cdot 2ss' + 2kx_0(K+k) \cdot s'\right] \cdot \left(s + \frac{kx_0}{K+k}\right) - N \cdot s' \\ O = (K+k) \cdot m_T \cdot \omega^2 \cdot 2 \cdot (s''^2 + s' \cdot s''') + (k^2 + 2 \cdot k \cdot K) \cdot 2 \cdot (s'^2 + s \cdot s'') + 2 \cdot k \cdot x_0 \cdot (K+k) \cdot s'' \\ x'' = s'' - \dfrac{\left[O \cdot \left(s + \frac{kx_0}{K+k}\right) - N \cdot s''\right] \cdot \left(s + \frac{kx_0}{K+k}\right) - M \cdot 2 \cdot s'}{2 \cdot (K+k)^2 \cdot \left(s + \frac{kx_0}{K+k}\right)^3} \end{cases} \tag{22}$$

$$\ddot{x} = x'' \cdot \omega^2 + x' \cdot \varepsilon \tag{23}$$

In the Figure 8 one can see the cam profile and in Fig. 9 the dynamic diagram.
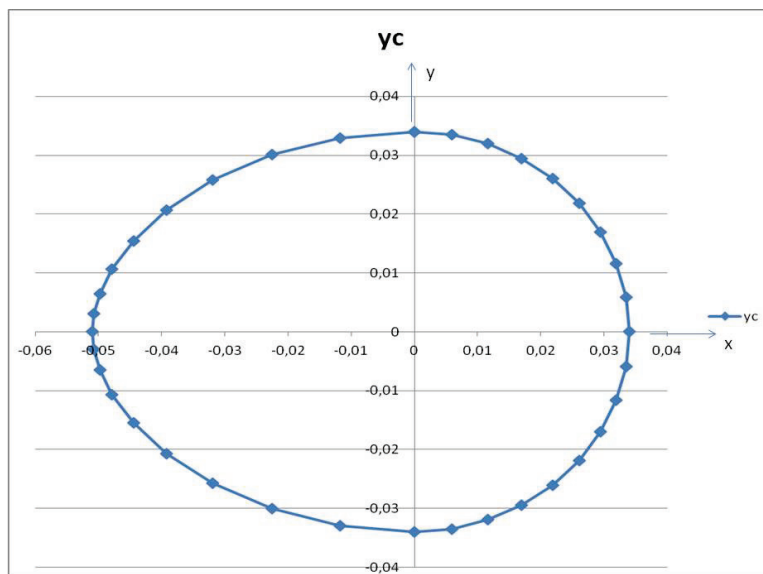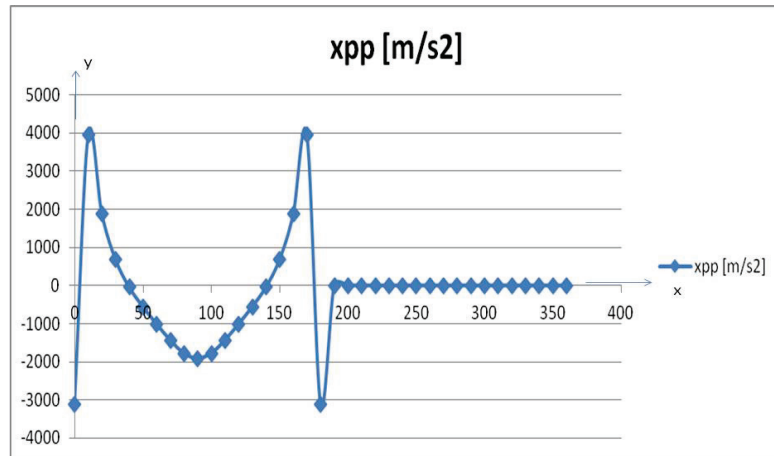

Fig. 8. The cam profile

Fig. 9. The dynamic diagram

The calculation program used for modeling and numerical simulations is presented in the appendix.

8   Conclusions

In this work, one presents the dynamic, original, machine motion equations. The equation of motion of the machine that generates the angular speed of the shaft (which varies with position and rotation speed) is obtained by conservation kinetic energy of the machine. An additional variation of angular speed is added by multiplying by the coefficient dynamic (generated by the forces out of mechanism). Kinetic energy conservation shows angular speed variation (from the main shaft) with inertial masses, while the dynamic coefficient introduces the variation of w with forces acting in the mechanism. The first movement equation of the machine takes the initial forms (system 2) and the final forms (systems 3-4).

The second machine equation is determined by the derivation of the first machine equation in function of the time (system 5). One determines then the dynamics of the classical distribution at an Otto engine. An important way to reduce losses of heat engines is how to achieve a good camshaft (a good distribution) mechanism. The profile synthesis must be made dynamic. The presented relationships permit this.

Nomenclature

J^*	is the moment of inertia (mass or mechanical) reduced to the camshaft
J^*_{Max}	is the maximum moment of inertia (mass or mechanical) reduced to the camshaft
J^*_{min}	is the minimum moment of inertia (mass or mechanical) reduced to the camshaft
J^*_m	is the average moment of inertia (mass or mechanical, reduced to the camshaft)
$J^{*\,\prime}$	is the first derivative of the moment of inertia (mass or mechanical, reduced to the camshaft) in relation with the φ angle
η_i	is the momentary efficiency of the cam-pusher mechanism
η	is the mechanical yield of the cam-follower mechanism

τ	is the transmission angle
δ	is the pressure angle
s	is the movement of the pusher
h	is the follower stroke $h=s_{max}$
s'	is the first derivative in function of φ of the tappet movement, s
s''	is the second derivative in raport of φ angle of the tappet movement, s
s'''	is the third derivative of the tappet movement s, in raport of the φ angle
x	is the real, dynamic, movement of the pusher
x'	is the real, dynamic, reduced tappet speed
x''	is the real, dynamic, reduced tappet acceleration
$\ddot{x}$	is the real, dynamic, acceleration of the tappet (valve).
$v_{\tau} \equiv \dot{s}$	is the normal (cinematic) velocity of the tappet
$a_{\tau} \equiv \ddot{s}$	is the normal (cinematic) acceleration of the tappet
φ	is the rotation angle of the cam (the position angle)
K	is the elastic constant of the system
k	is the elastic constant of the valve spring
x_0	is the valve spring preload (pretension)
m_c	is the mass of the cam
m_T	is the mass of the tappet
ω_m	the nominal angular rotation speed of the cam (camshaft)
n_c	is the camshaft speed
$n=n_m$	is the motor shaft speed $n_m=2n_c$
ω	is the dynamic angular rotation speed of the cam
ε	is the dynamic angular rotation acceleration of the cam
r_0	is the radius of the base circle
$\rho=r$	is the radius of the cam (the position vector radius)
θ	is the position vector angle
$x=x_c$ and $y=y_c$	are the Cartesian coordinates of the cam
D	is the dynamic coefficient
$\dot{D}$	is the derivative of D in function of the time
D'	is the derivative of D in function of the position angle of the camshaft, φ
Fm	is the motor force
Fr	is the resistant force.

REFERENCES

[1]- P. Antonescu, F.I.T. Petrescu, O. Antonescu, Contributions to the Synthesis of The Rotary Disc-Cam Profile, In: Proceedings of the VIII-th International Conference on the Theory of Machines and Mechanisms, Liberec, Czech Republic, 2000, pp. 51-56.

[2]- P. Antonescu, M. Oprean, F.I.T. Petrescu, The dynamic analysis of the distribution mechanisms cams. In: Proceedings of the 7th National Symposium of Industrial Robots and Spatial Mechanisms, Vol. 3, Bucharest, 1987.

[3]- R. Aversa, R.V. Petrescu, A. Apicella, F.I.T. Petrescu, JK. Calautit, M.M. Mirsayar, R. Bucinell, F. Berto, B. Akash, Something about the V Engines Design. Am. J. Appl. Sci. 14(1) (2017) 34-52. doi:10.3844/ajassp.2017.34.52

[4]- R. Aversa, R.V. Petrescu, A. Apicella, F.I.T. Petrescu, Nano-Diamond Hybrid Materials for Structural Biomedical Application, Am. J. Biochem. Biotech. 13(1) (2017) 34-41. doi:10.3844/ajbbsp.2017.34.41

[5]- R. Aversa, D. Parcesepe, R.V. Petrescu, F. Berto, G. Chen, F.I.T. Petrescu, F. Tamburrino, A. Apicella, Processability of Bulk Metallic Glasses. Am. J. Appl. Sci. 14(2) (2017) 294-301. doi:10.3844/ajassp.2017.294.301

[6]- R. Aversa, R.V. Petrescu, B. Akash, R. Bucinell, J. Corchado, F. Berto, MM. Mirsayar, G. Chen, S. Li, A. Apicella, F.I.T. Petrescu, Something about the Balancing of Thermal Motors. Am. J. Eng. Appl. Sci. 10(1) (2017) 200-217. doi:10.3844/ajeassp.2017.200.217

[7]- R. Aversa, R.V. Petrescu, A. Apicella, F.I.T. Petrescu, A Dynamic Model for Gears. Am. J. Eng. Appl. Sci. 10(2) (2017) 484-490. doi:10.3844/ajeassp.2017.484.490

[8]- R. Aversa, D. Parcesepe, R.V. Petrescu, G. Chen, F.I.T. Petrescu, F. Tamburrino, A. Apicella, Glassy Amorphous

Metal Injection Molded Induced Morphological Defects. Am. J. Appl. Sci. 13(12) (2016) 1476-1482. doi:10.3844/ajassp.2016.1476.1482

[9]- R. Aversa, R.V. Petrescu, F.I.T. Petrescu, A. Apicella, Smart-Factory: Optimization and Process Control of Composite Centrifuged Pipes. Am. J. Appl. Sci. 13(11) (2016) 1330-1341. doi:10.3844/ajassp.2016.1330.1341

[10]- R. Aversa, F. Tamburrino, R.V. Petrescu, F.I.T. Petrescu, M. Artur, G. Chen, A. Apicela, Biomechanically Inspired Shape Memory Effect Machines Driven by Muscle like Acting NiTi Alloys. Am. J. Appl. Sci. 13(11) (2016) 1264-1271. doi:10.3844/ajassp.2016.1264.1271

[11]- F. Berto, R.V. Petrescu, F.I.T. Petrescu, A Review of Recent Results on 3D Effects. Am. J. Eng. Appl. Sci. 9(4) (2016) 1247-1260. doi:10.3844/ajeassp.2016.1247.1260

[12]- F. Berto, R.V. Petrescu, F.I.T. Petrescu, Three-Dimensional in Bonded Joints: A Short Review. Am. J. Eng. Appl. Sci. 9(4) (2016) 1261-1268. doi:10.3844/ajeassp.2016.1261.1268

[13]- F. Berto, A. Gagani, R.V. Petrescu, F.I.T. Petrescu, Key-Hole Notches in Isostatic Graphite: A Review of Some Recent Data. Am. J. Eng. Appl. Sci. 9(4) (2016) 1292-1300. doi:10.3844/ajeassp.2016.1292.1300

[14]- F. Berto, A. Gagani, R. Aversa, R.V. Petrescu, A. Apicela, F.I.T. Petrescu, Multiaxial Fatigue Strength to Notched specimens made of 40CrMoV13.9. Am. J. Eng. Appl. Sci. 9(4) (2016) 1269-1291. doi:10.3844/ajeassp.2016.1269.1291

[15]- M.M. Mirsayar, V.A. Joneidi, R.V. Petrescu, F.I.T. Petrescu, F. Berto, Extended MTSN criterion for fracture analysis of soda lime glass. Eng. Fract. Mech. 178 (2017) 50–59. doi:10.1016/j.engfracmech.2017.04.018

[16]- R.V. Petrescu, R. Aversa, B. Akash, R. Bucinell, J. Corchado, F. Berto, MM. Mirsayar, JK. Calautit, A. Apicela, F.I.T. Petrescu, Yield at Thermal Engines Internal Combustion. Am. J. Eng. Appl. Sci. 10(1) (2017) 243-251. doi:10.3844/ajeassp.2017.243.251

[17]- R.V. Petrescu, R. Aversa, B. Akash, R. Bucinell, J. Corchado, F. Berto, MM. Mirsayar, JK. Calautit, A. Apicela, F.I.T. Petrescu, Forces at Internal Combustion Engines. Am. J. Eng. Appl. Sci. 10(2) (2017) 382-393. doi:10.3844/ajeassp.2017.382.393

[18]- R.V. Petrescu, R. Aversa, B. Akash, R. Bucinell, J. Corchado, F. Berto, MM. Mirsayar, A. Apicela, F.I.T. Petrescu, Gears-Part I. Am. J. Eng. Appl. Sci. 10(2) (2017) 457-472. doi:10.3844/ajeassp.2017.457.472

[19]- R.V. Petrescu, R. Aversa, B. Akash, R. Bucinell, J. Corchado, F. Berto, M.M. Mirsayar, A. Apicella, F.I.T. Petrescu, Gears-Part II. Am. J. Eng. Appl. Sci. 10(2) (2017) 473-483. doi:10.3844/ajeassp.2017.473.483

[20]- R.V. Petrescu, R. Aversa, B. Akash, R. Bucinell, J. Corchado, F. Berto, MM. Mirsayar, A. Apicela, F.I.T. Petrescu, Cam-Gears Forces, Velocities, Powers and Efficiency. Am. J. Eng. Appl. Sci. 10(2) (2017) 491-505.doi: 10.3844/ajeassp.2017.491.505

[21]- R.V. Petrescu, R. Aversa, B. Akash, R. Bucinell, J. Corchado, F. Berto, MM. Mirsayar, S. Kosaitis, T. Abu-Lebdeh, A. Apicela, F.I.T. Petrescu, Dynamics of Mechanisms with Cams Illustrated in the Classical Distribution. Am. J. Eng. Appl. Sci. 10(2) (2017) 551-567. doi:10.3844/ajeassp.2017.551.567

[22]- R.V. Petrescu, R. Aversa, B. Akash, R. Bucinell, J. Corchado, F. Berto, MM. Mirsayar, S. Kosaitis, T. Abu-Lebdeh, A. Apicela, F.I.T. Petrescu, Testing by Non-Destructive Control, Am. J. Eng. Appl. Sci. 10(2) (2017) 568-583. doi:10.3844/ajeassp.2017.568.583

[23]- R.V. Petrescu, R. Aversa, A. Apicela, F.I.T. Petrescu, Transportation Engineering. Am. J. Eng. Appl. Sci. 10(3) (2017) 685-702. doi:10.3844/ajeassp.2017.685.702

[24]- R.V. Petrescu, R. Aversa, S. Kozaitis, A. Apicela, F.I.T. Petrescu, The Quality of Transport and Environmental Protection, Part I. Am. J. Eng. Appl. Sci. 10(3) (2017) 738-755. doi:10.3844/ajeassp.2017.738.755

[25]- F.I.T. Petrescu, J.K.Calautit, MM.Mirsayar, D. Marinkovic, Structural Dynamics of the Distribution Mechanism with Rocking Tappet with Roll. Am. J. Eng. Appl. Sci. 8(4) (2015) 589-601. doi:10.3844/ajeassp.2015.589.601

[26]- F.I.T. Petrescu, R.V. Petrescu, Otto Motor Dynamics. Geintec-Gestao Inovacao e Tecnologias, 6(3) (2016) 3392-3406. doi:10.7198/geintec.v6i3.373

[27]- F.I.T. Petrescu, R.V. Petrescu, Cam Gears Dynamics in the Classic Distribution. Ind. J. Manag.Prod. 5(1) (2014) 166-185. doi:10.14807/ijmp.v5i1.133

[28]- F.I.T. Petrescu, R.V. Petrescu, An Algorithm for Setting the Dynamic Parameters of the Classic Distribution Mechanism. Int. Rev. Model. Simul. 6(5) (2013) 1637-1641.

[29]- F.I.T. Petrescu, R.V. Petrescu, Dynamic Synthesis of the Rotary Cam and Translated Tappet with Roll. Int. Rev. Model. Simul. 6(2) (2013) 600-607.

[30]- F.I.T. Petrescu, R.V. Petrescu, Cams with High Efficiency. Int. Rev. Mech. Eng. 7(4) (2013) 599-606.

[31]- F.I.T. Petrescu, R.V. Petrescu, Forces and Efficiency of Cams. Int. Rev. Mech. Eng. 7(3) (2013) 507-511.

[32]- F.I.T. Petrescu, R.V. Petrescu, Dinamica mecanismelor de distributie. Create Space publisher, USA, (Romanian version), 2011. ISBN 978-1-4680-5265-7

[33]- F.I.T. Petrescu, R.V. Petrescu, Contributions at the dynamics of cams. In: Proceedings of the Ninth IFToMM International Symposium on Theory of Machines and Mechanisms, Bucharest, Romania, 2005, Vol. I, p. 123-128.

[34]- F.I.T. Petrescu, R.V. Petrescu, Determining the dynamic efficiency of cams. In: Proceedings of the Ninth IFToMM International Symposium on Theory of Machines and Mechanisms, Bucharest, Romania, 2005, Vol. I, p. 129-134.

[35]- F.I.T. Petrescu, Geometrical Synthesis of the Distribution Mechanisms. Am. J. Eng. Appl. Sci. 8(1) (2015) 63-81. doi:10.3844/ajeassp.2015.63.81

[36]- F.I.T. Petrescu, Machine Motion Equations at the Internal Combustion Heat Engines. Am. J. Eng. Appl. Sci. 8(1) (2015) 127-137. doi:10.3844/ajeassp.2015.127.137

[37]- F.I.T. Petrescu, Bazele analizei şi optimizării sistemelor cu memorie rigidă – curs şi aplicaţii. Create Space publisher, USA, (Romanian edition), 2012. ISBN 978-1-4700-2436-9

[38]- F.I.T. Petrescu, Teoria mecanismelor – Curs si aplicatii (editia a doua). Create Space publisher, USA, (Romanian version), 2012. ISBN 978-1-4792-9362-9

[39]- J. Syed, A. Dharrab, M. Zafa, E. Khand, R. Aversa, R.V. Petrescu, A. Apicela, F.I.T. Petrescu, Influence of Curing Light Type and Staining Medium on the Discoloring Stability of Dental Restorative Composite. Am. J. Biochem. Biotech. 13(1) (2017) 42-50. doi:10.3844/ajbbsp.2017.42.50

[40]- K.Hain, Optimization of a cam mechanism to give good transmissibility maximal output angle of swing and minimal acceleration. J. Mechanisms 6(4) (1971) 419-434. doi:10.1016/0022-2569(71)90044-9

[41]- F. Giordana, V. Rognoni, G. Ruggieri, On the influence of measurement errors in the Kinematic analysis of cam. Mechanism Mach. Theory 14(5) (1979) 327-340. doi:10.1016/0094-114X(79)90019-3

[42]- P. Antonescu, F.I.T. Petrescu, Analytical method of synthesis of cam mechanism and flat stick. In: Proceedings of the Fourth International Symposium on Theory and Practice of Mechanisms, Vol. III-1, Bucharest, 1985.

[43]- P. Antonescu, F.I.T. Petrescu, D. Antonescu, Sinteza geometrică a mecanismului rotativ de camă şi balansier. SYROM'97, Bucureşti, 1997.

[44]- J. Angeles, C. Lopez-Cajun, Optimal synthesis of cam mechanisms with oscillating flat-face followers. Mechanism Mach. Theory 23(1) (1988) 1-6. doi:10.1016/0094-114X(88)90002-X

[45]- D. Taraza, N.A. Henein, W. Bryzik, The Frequency Analysis of the Crankshaft's Speed Variation: A Reliable Tool for Diesel Engine Diagnosis. J. Eng. Gas Turbines Power 123(2) (2001) 428-432. doi:10.1115/1.1359479

[46]- J.L. Wiederrich, B. Roth, Design of low vibration cam profiles. In: Cams and Cam Mechanisms. Ed. J. Rees Jones, MEP, London and Birmingham, Alabama, 1974.

[47]- G.F. Fawcett, J.N. Fawcett, Comparison of polydyne and non polydyne cams. In: Cams and cam mechanisms. Ed. J. Rees Jones, MEP, London and Birmingham, Alabama, 1974.

[48]- J.R. Jones, J.E. Reeve, Dynamic response of cam curves based on sinusoidal segments. In: Cams and cam mechanisms. Ed. J. Rees Jones, MEP, London and Birmingham, Alabama. 1974

[49]- D. Tesar, G.K. Matthew, The design of modeled cam systems. In: Cams and cam mechanisms, Ed. J. Rees Jones, MEP, London and Birmingham, Alabama, 1974

[50]- I. Sava, Contributions to Dynamics and Optimization of Income Mechanism Synthesis. Ph.D. Thesis, I.P.B., 1970

[51]- M.P. Koster, The effects of backlash and shaft flexibility on the dynamic behavior of a cam mechanism. In: Cams and cam mechanisms, Ed. J. Rees Jones, MEP, London and Birmingham, Alabama, 1974.

[52]- P. Antonescu, F.I.T. Petrescu, Contributions to kineto elastodynamic analysis of distribution mechanisms. SYROM 89, Bucharest, 1989

Appendix A. Calculation program used for modeling and numerical simulations

	A	B
1	h[mm]	0,017
2	φ[deg]	0
3	φ[rad]	=B2*PI()/180
4	s	=B1/2*(1-COS(2*B3))
5	s'	=B1*SIN(2*B3)

6	s"	=2*B1*COS(2*B3)
7	r0 [mm]	0,034
8	φu[rad]	=PI()/2
9	φ[deg]	0
10	s [m]	=B4
11	s' [m]	=B5
12	s" [m]	=B6
13	s''' [m]	=-(PI())^3/2*B1/B8^3*SIN(PI()*B3/B8)
14	xc	=-(B7+B10)*SIN(B3)-B11*COS(B3)
15	yc	=(B7+B10)*COS(B3)-B11*SIN(B3)
16	Mc [kg]	=0,2
17	mT [kg]	=0,1
18	n [rot/min]	5500
19	ω_m [s^{-1}]	=PI()*B18/60
20	ω_m^2 [s^{-2}]	=B19^2
21	C1 [kgm2]	=B16*B7^2+B16*B1^2/8+B16/2*B7*B1+ B16/8*(PI())^2*B1^2/B8^2+B17/4*(PI())^2*B1^2/B8^2
22	Ex1 [kgm2]	=B16*B7^2+B16*B10^2+2*B16*B7*B10+B16*B11^2+2*B17*B11^2
23	Ex1'/2 [kgm2]	=B16*B10*B11+B16*B7*B11+B16*B11*B12+2*B17*B11*B12
24	ω^2 [s^{-2}]	=B20*B21/B22
25	ω [s^{-1}]	=SQRT(B24)
26	e [s^{-2}]	=-B21*B23*B20/B22^2
27	sin^{2}t	=B11^2/((B7+B10)^2+B11^2)
28	η	=SUM(B27:T27)/19
29	t [rad]	=ASIN(B11/SQRT((B7+B10)^2+B11^2))
30	tmax [rad]	=MAX(B29:T29)
31		
32	x0 [m]	0,03
33	φ[deg]	=B9
34	s_{pp} [ms^{-2}]	=B12*B24+B11*B26
35	K [N/m]	=5000000
36	k [N/m]	20000
37	x" [m]	=B12-(((((B35+B36)*B17*B24*2*(B12^2+B11*B13)+(B36^2+2*B36*B35)*2* (B11^2+B10*B12)+2*B36*B32*(B35+B36)*B12)* (B10+B36*B32/(B35+B36))+((B35+B36)*B17*B24*2*B11*B12+ (B36^2+2*B36*B35)*2*B10*B11+2*B36*B32*(B35+B36)*B11)*B11-B12* ((B35+B36)*B17*B24*B11^2+(B36^2+2*B36*B35)*B10^2+2*B36*B32* (B35+B36)*B10)-B11*((B35+B36)*B17*B24*2*B11*B12+ (B36^2+2*B36*B35)*2*B10*B11+2*B36*B32*(B35+B36)*B11))* (B10+B36*B32/(B35+B36))^2-(((B35+B36)*B17*B24*2*B11*B12+ (B36^2+2*B36*B35)*2*B10*B11+2*B36*B32*(B35+B36)*B11)* (B10+B36*B32/(B35+B36))-((B35+B36)*B17*B24*B11^2+ (B36^2+2*B36*B35)*B10^2+2*B36*B32*(B35+B36)*B10)*B11) *2*(B10+B36*B32/(B35+B36))*B11/ (2*(B35+B36)^2*(B10+B36*B32/(B35+B36))^4)
38	x' [m]	=B11-(((B35+B36)*B17*B24*2*B11*B12+(B36^2+2*B36*B35)*2*B10*B11+ 2*B36*B32*(B35+B36)*B11)*(B10+B36*B32/(B35+B36))- ((B35+B36)*B17*B24*B11^2+(B36^2+2*B35*B36)*B10^2+ 2*B36*B32*(B35+B36)*B10)*B11)/(2*(B35+B36)^2*(B10+B36*B32/(B35+B36))^2)
39	tantau	=TAN(B29)
40	tau[deg]	=B29*180/PI()
41		
42	φ[deg]	=B33
43	xpp [m/s2]	=B37*B24+B38*B26
44		